Nathan Coleman[1]
Department of Mechanical Engineering,
Brigham Young University,
Provo, UT, USA
email: nathan.coleman@jhuapl.edu

Jacob Sutton
Department of Mechanical Engineering,
Brigham Young University,
Provo, UT, USA
email: jas546@byu.edu

Ivy Running
Department of Mechanical Engineering,
Brigham Young University,
Provo, UT, USA email:
ivy_oveson@byu.edu

Spencer Magleby
Department of Mechanical Engineering,
Brigham Young University,
Provo, UT, USA
email: magleby@byu.edu

Larry L. Howell
Department of Mechanical Engineering,
Brigham Young University,
Provo, UT, USA
email: lhowell@byu.edu

Modeling and Analysis of Inter-Panel Slipping for the Design of Rolled Gossamer Arrays

Many deployable satellite systems benefit from having low mass and high surface area, which has led to the proliferation of gossamer structures in space-based applications. Gossamer structures are characterized by lightweight, low stiffness membranes, which can flex and roll to compactly stow. An effect of rolling a gossamer structure is that there is tangential separation along adjacent panels as they roll, resulting in relative motion between panels. To aid designers in predicting and accommodating this motion, a method for modeling the slippage between adjacent panels that occurs while rolling is presented. This analytical slippage model and algorithm is a function of 1) the number of panels, 2) the thickness of each panel, 3) the length of each panel, and 4) the minimum bend radius of the material. It is shown that the thickness and length have a positive correlation with increased slippage, whereas the number of panels and minimum bend radius have a negative correlation with increased slippage. This model allows designers to predict both the magnitude of slippage that occurs where panels meet, as well as the relative range of slippage that occurs within the whole pattern. With these predictions, an appropriate strategy can be selected for accommodating this motion.

Keywords: Gossamer, Origami, Compliant Mechanisms, Satellite, Deployable Arrays

1 Introduction

The usage of space-based satellite systems has become increasingly common and the rate of new objects being launched into space has risen dramatically over the past few years [1]. As designers strive to improve the capabilities of satellites, demand has grown for achieving greater surface areas coupled with smaller volumes. Two tools that have aided designers in improving the mechanical capability and performance of space-based structures are origami and compliant mechanisms.

Origami has its roots in the ancient art of paper folding, and is useful as a basis for design because it allows designers to couple the motion of various parts of the system, reducing the degrees-of-freedom in the system and consequently reducing the number of actuators required. Origami has recently been used in the design of single degree-of-freedom aerodynamic control surfaces, robots, and soft actuators [2–6], and it has proved to be a versatile method of designing mechanical systems.

Compliant mechanisms allow for motion through the deflection of one or more of their members, giving them the ability to accommodate folding motion without increasing the number of parts in the design [7]. This is particularly useful in addressing the demands of space-based systems, which are often restricted by mass and volume requirements. Recent research demonstrates the value of compliant mechanisms in space-based applications, such as for docking joints for CubeSats, constant force mechanisms, and robotic grippers [8–11].

An intersection between origami and compliant mechanisms that is particularly well suited to addresses the requirements of mass and volume is gossamer structures, which are typically lightweight, thin, and have a low stiffness. Gossamer structures often combine the folded structures seen in origami with the mechanical capability of compliant mechanisms. Gossamer structures have been used by space agencies as far back as the 1950s [12], and their development continues to generate new research and applications, including inflatable, ribbed, tensioned, parabolic, wrinkled, reflectors, sails, solar arrays, and optical gossamer structures [13–21].

Inspired by the precision requirements of reflectarray antennae, this research focuses on gossamer arrays that reduce the wrinkling that commonly occurs in stowed membranes [22] by rolling sections of the array [14,15,23]. Gossamer structures are structures which are typically systems constructed from flexible membranes, which have the advantages of being lightweight, flexible, and easily stowable, such as the example shown in Fig. 1. Examples of gossamer structures include solar sails and sun shades. This work characterizes the relative motion in rolled gossamer arrays, proposes a model for simulating this behavior, uses the model to show trade offs and trends when changing competing design parameters, and shows an implementation of hinges that accommodate this motion.

[1]Corresponding Author.
October 3, 2024

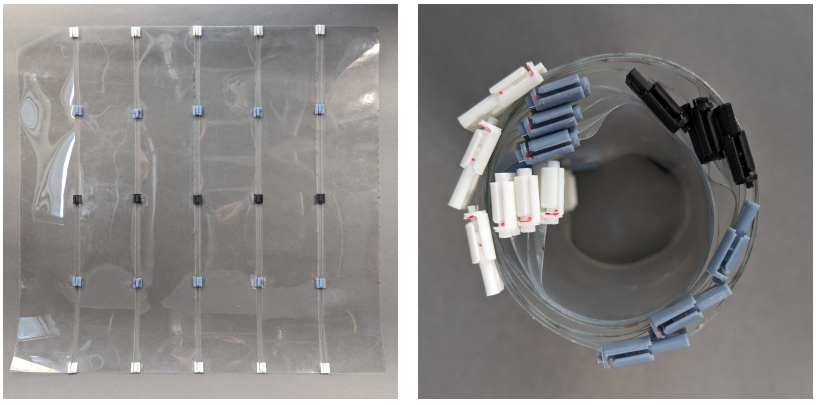

(*a*) (*b*)

Fig. 1 Example implementation of a gossamer pattern. (a) Deployed state, showing how a design may be visualized as a series of strips connected by hinges. In this example, there are 5 hinges connecting each set of adjacent panels. (b) Rolled. This model is shown in the an additional possible rolled state in Fig.8.

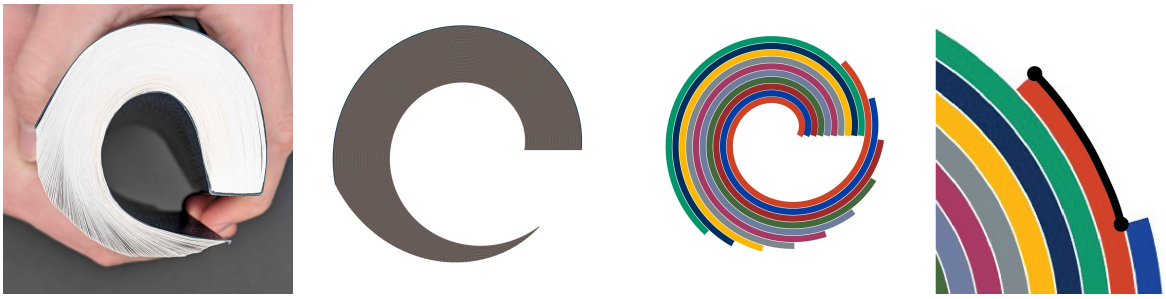

(*a*) (*b*) (*c*) (*d*)

Fig. 2 Example figure of slipping that occurs during rolling. (a) Rolled book showing slipping between pages. (b) Simulation model of book slippage. Model has 600 panels each with a thickness of 0.02 mm, a total length of 120 mm, and a minimum bend radius of 15 mm, as measured on the book. Because each membrane is so thin, it is difficult to distinguish layers in this example; however the model can be seen to align closely with the physical model, validating the rolling model used. (c) Simple example model to show individual panels. (d) Close-up showing slipping that occurs on the same point between panels in black.

2 Background

One of the main challenges of designing rolled gossamer structures is that buckling and plastic deformation occurs if slipping is not allowed between adjacent sections of the membrane. The terms "panel" and "strips" will be used interchangeably to refer to these adjacent sections. Panel slipping occurs in patterns using rolled membranes because the membrane layers on the outer part of the roll have further to travel than the inner membrane layers. Although the difference in diameter between the inner and outer layers may be small, it can have significant consequences to the alignment of the satellite elements, negatively impacting capability and performance of an otherwise impressive array. A simple example of the slippage between membrane layers can be observed by rolling up any softcover book; pages can be seen to immediately separate from each other as shown in Fig. 2(*a*). However, this effect makes creases in a continuous folded membrane problematic, as they do not allow for relative motion in the direction of slippage required for rolling as the pages of a book do, leading to wrinkling and deformations in the design.

This work aims to characterize the slipping motion in patterns made with parallel rectangular strips, such that slippage can be accurately predicted and accommodated. If the amount of slippage required for a given array can be known beforehand, designers can implement techniques to allow for sufficient motion and preserve the performance of the array. As such, effects of changing model parameters are shown, and trends which may be used by designers to predict behavior are illustrated.

3 Model

Gossamer patterns are defined by a variety of variables generally based around their required performance; these may include length and width dimensions, thickness, number of panels, surface characteristics, material properties, and so on. The method proposed predicts the amount of slippage that occurs using four of these, which are the number of panels, the thickness of each panel, the length of each panel, and the minimum bend radius of the material. A fifth variable may be included, which is how the array is rolled. Three simple rolling models are shown for illustration in Fig. 3, however, many other models may be used, such as those shown by Arya et al. [24]. Additionally, future work could apply the principles and methods discussed to predict slip in other rolled patterns created with non-uniform panels. In rolled gossamer patterns, panels are connected continuously along their creases. For the purposes of visualizing and discretizing the slip, the pattern can be imagined as separate strips connected by a discrete number of hinges along the length of the strip, such as the example shown in Fig.1. This allows the slip at each hinge location to be quantified, although in a continuous crease joining two strips, this slip could be represented by a continuous curve. In Fig. 4(*a*) these hinge locations are represented by circles

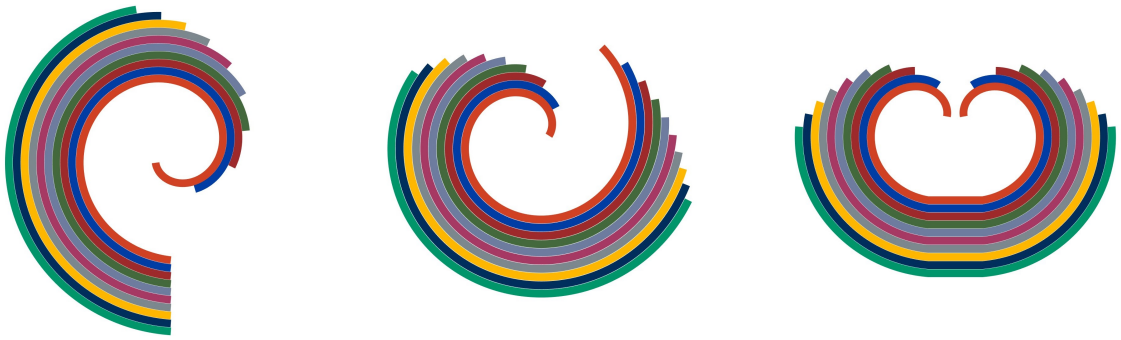

(*a*) (*b*) (*c*)

Fig. 3 Additional rolling models. (a) Exterior aligned, where the outer most edge of each sheet is kept aligned to its adjacent panel. (b) Centered, where the initial angle of each panel in the roll has been adjusted to balance the amount of slipping on each end of a panel, such that the slip on each end is kept equal. This reduces the maximum magnitude of the slippage on any panel. (c) Double roll, where each end is rolled towards the middle.

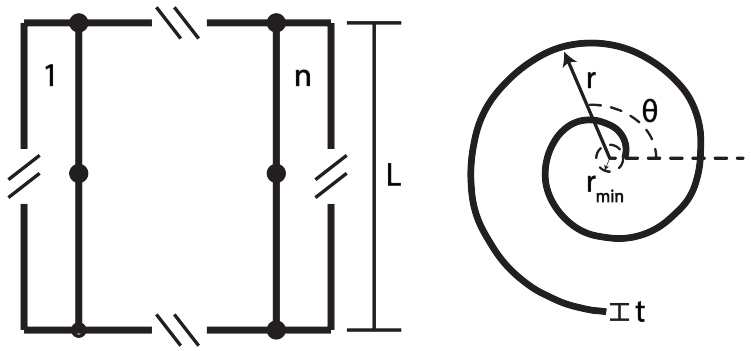

(*a*) (*b*)

Fig. 4 General Array Nomenclature. (a) Number of panels, length, and hinges definition figure. Hinges locations are shown as circles, indicating the point on each panel where slip is being measured. Note that the width of each panel does not affect the slipping between panels, as it is into the plane and does not affect the arc length being measured. (b) Thickness and minimum radius definition.

along the length of each strip. It should be noted that this model constrains that each panel is rolled tightly and that gaps are not allowed between panels[2]. The four primary variables used are defined as follows:

- **Number of panels (n)**: Any flat array may be divided into n sections. In this work, arrays which are divided into strips are considered, where the width of each strip is defined by the width of the array divided by the number of strips, and the length of each strip is equal to the length of the array, as illustrated in Fig. 4(*a*).
- **Thickness of each panel (t)**: The thickness of the array. Depending on the purpose of the array, this may be non-uniform, however in this work each panel is considered as having a uniform, equal thickness. Arrays that have an irregular surface may be found to have an effective thickness which can be used in this model; alternatively a more complex implementation could consider each unique thickness separately.
- **Length of each panel (L)**: The length of the array. This parameter is the same for each panel.
- **Minimum bend radius** (r_{min}): This is defined by the material properties of the material being rolled, and determines how tightly the array can roll.

In this work, results from the interior aligned model (where the interior edge of each panel is kept aligned), shown in Fig. 2(*c*) will be shown, because it is the simplest model which illustrates the trends and trade-offs of changing each parameter. Note however, the results shown apply to each of the alternative models shown in Fig. 3. The exterior aligned model (where the exterior edges of each panel are kept aligned), shown in Fig. 3(*a*), keeps all of the panel edges on the exterior of the roll aligned and has the edges on the interior of the roll slip relative to each other. The centered roll model, shown in Fig. 3(*b*), rolls such that the amount of slipping on each end of a panel is kept equal to reduce the maximum magnitude of the slippage on a panel. Rather than having zero slip on one edge and a maximum slip on the opposite end, each edge experiences half of the maximum slip. There exists a location between each panel where there is no relative slip, however it is more complicated to predict, and so in practice, the double roll is more intuitive and would most likely be a

[2]To roll a pattern less tightly in this model, the minimum bend radius of the pattern should be increased. This can also be used to simulate the effect of rolling or unrolling the pattern to understand how the slip between panels changes during these events.

better rolling candidate than the centered roll model. The double roll model, shown in Fig. 3(*c*), rolls both outside edges towards the middle, such that the exterior edges slip symmetrically.

3.1 Slippage Model. In the following model, polar coordinates were used, where the radius is a function of the input angle. The model is implemented by the following algorithm.

Algorithm 1 Rolled Interior Aligned Model Algorithm

procedure FIND POSITIONS OF PANELS IN ROLL
  Initialize variables L, t, n, r_{min}
  for $i \rightarrow 1$ to n **do**
    $\theta_{final,i} = \theta_{final,i-1} + d\theta$
    $l = \int_0^{\theta_{final,i}} \sqrt{r^2 + \left(\frac{dr}{d\theta}\right)^2}\, d\theta$
    while $l < L$ **do**
      $\theta_{final,i} += d\theta$
      $l = \int_0^{\theta_{final,i}} \sqrt{r^2 + \left(\frac{dr}{d\theta}\right)^2}\, d\theta$
    end while
  end for
  for $i \rightarrow 1$ to n **do**
    Create vector from $0 \rightarrow \theta_{final,i}$ for panel i
  end for
  for $i \rightarrow 1$ to n **do**
    Calculate radii at each point in panel i using
    $r = r_{min} + (i-1)t + (\frac{t}{2})f + [\frac{\theta}{2\pi}nt]$
  end for
  return θ and radii vectors
end procedure

This method verifies that each panel is of the length defined, as shown in Fig. 2(*c*). Because the slip between panels is being characterized as points set a prescribed distance away from each edge, the location of each “hinge" in the rolled state my be found using a similar method to Algorithm 1, however instead of finding a θ_{final} for each panel which resulting in the panel being the correct length, a θ_d which corresponds to each hinge location is found, such that the length is equal to the hinge’s distance from the edge of the pattern. This allows the hinge points in the rolled state to be found, and the distance between the same points on adjacent panels to be measured, which is then used to define the slip that occurs at each location. An example of an interior aligned model with hinges is shown in Fig. 5. Fig. 5(*b*) shows the distance between adjacent panels at each hinge location, indicating the amount of slip that is required at each location to enable the gossamer to roll.

The length of a polar curve can be found by

$$l = \int_{\theta_{initial,i}}^{\theta_{final,i}} \sqrt{r^2 + \left(\frac{dr}{d\theta}\right)^2}\, d\theta \tag{1}$$

and the radius of any point is defined by the equation

$$r = r_{min} + (i-1)t + (\frac{t}{2})f + [\frac{\theta}{2\pi}nt]. \tag{2}$$

This equation has several parts. The first three terms consist of determining the initial radius of any sheet, and the fourth term adds the effect of the angle at which the particular coordinate is at. The initial radius of each panel is affected by several factors, such as the minimum bend radius, how many panels are below it in the pattern, as well as the thickness of the material being rolled. The first term (r_{min}) accommodates the minimum bend radius, the second term ($(i-1)t$) adds the thickness of all of the panels closer to the center than the sheet being found, and the third term ($(\frac{t}{2})f$) is a factor to find either the top, middle, or bottom surface location of any panel, where $f = 1, 0$, or -1 for the top, middle, and bottom surfaces, respectively. The fourth term ($[\frac{\theta}{2\pi}nt]$) adds to the radius in proportion to the angle at which any point is at, using the assumption that the radius increases the total thickness of all panels in each full rotation. This is intuitive, as the bottom surface of the innermost panel in a pattern will be in contact with the top surface of the outermost panel when it has made a full rotation. If the radius were smaller after one rotation, the panels would interfere with each other and it would not be able to roll. While some rolled patterns do not make a full rotation, such as that shown in Fig. 2(*b*), it is assumed that the radius is continually increasing with this same relationship. Fig. 2(*c*) shows how, after a rotation of 2π radians, the radius of the innermost panel has been offset from its original value by the sum of the thicknesses of the other panels.

By substituting Eq. 2 into Eq. 1, the analytical solution for the length of a sheet of material in a rolled pattern can be found using the following equations:

$$A = n\,t \tag{3}$$

$$B = r_{min} + t\ (i-1) \tag{4}$$

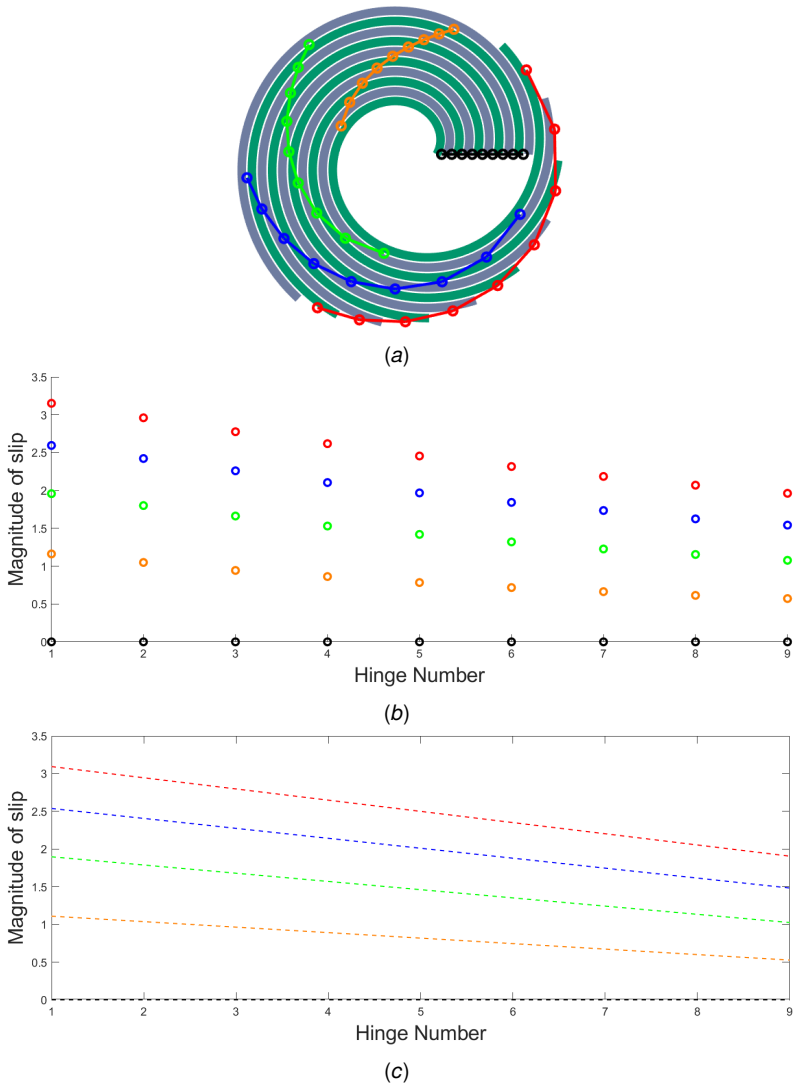

Fig. 5 Interior aligned model with five hinges. (a) Model with given parameters, with hinge locations shown halfway through the slip measured for adjacent panels. (b) Plot of the magnitude of slip required at each hinge location. (c) Linear fit to the slippage plot.

$$C = \frac{A^2}{4} + \pi^2 i^2 t^2 - 2\pi^2 i t^2 + \pi^2 t^2 \tag{5}$$

$$D = r_{min}^2 \pi^2 - 2 r_{min} t \pi^2 + 2 r_{min} i t \pi^2 \tag{6}$$

$$E = \sqrt{A^2 \theta^2 + A^2 + 4\pi A B \theta + 4\pi^2 B^2} \tag{7}$$

$$F = E\ (A\theta + 2\pi B) \tag{8}$$

$$G = \sqrt{A^2 \theta^2 + 4 B \pi A \theta + 4 C + 4 D} \tag{9}$$

$$l(\theta) = \left(\frac{1}{4 A \pi}\right)\left[F + A^2 \ln\left(\frac{A^2 \theta + A G + 2\pi A B}{2 A \pi}\right)\right] \tag{10}$$

4 Simulation Results

Using this model, the relative displacement between adjacent panels in a rolled pattern can be determined for any point along the panel. This allows for the prediction of the translational motion required when actuating these structures, which is particularly useful when determining appropriate hinges to incorporate into a design.

The four parameters outlined in Section 3 determine the final displacement of the rolled model. Using the model, the effect that each of these has on the final design and how to tailor each parameter to modify the overall slippage between panels can be determined.

To visualize the effect of slipping on the model, a number of hinges to be equally spaced along the panel are assigned, and then plot the relative displacement between panels at each hinge location. An example of this is shown in Fig. 5. It should be noted that a pattern with n panels will have $n-1$ hinges. In Fig. 5, each hinge location is defined by a distance away from the interior edge, and is represented by a unique color. This facilitates visualization of how the magnitude of the relative displacement between panels increases along each panel as it is further from the aligned edge, as well as how the relative displacement changes along a given hinge location for each panel which is further away from the center of the roll. The two primary parameters that will be used to quantify results are the maximum displacement found within a pattern, as well as the slope of a linear fit to the displacement of each hinge location. The maximum displacement is useful for quantifying how much parasitic motion needs to be incorporated into a design to accommodate slippage between panels. This affects the design of hinges in the pattern and strategies they use. For example, a pattern with a small maximum displacement may incorporate a compliant hinge that achieves precise behavior, while a pattern with more displacement may require a hinge which allows sliding between panels, such as that shown in Section 5. More relative displacement required between panels is similar to adding more degrees of freedom to the system, in that more motion and freedom into the system to achieve folding must be introduced. As such, minimizing the magnitude of relative motion between panels is preferred in the scope of this work.

An additional metric for determining the desirability of the configuration is the slope of a linear fit to the displacement along a hinge location. Finding a linear fit to each set of hinges defined by a hinge location allows the relative range of displacements which are required at each hinge location to be found. The displacement of each hinge location is illustrated in Fig. 5(*c*) by a line of each color. On this plot, many individual points can be seen, each of which represents an individual hinge in the pattern, and by minimizing the slope of the linear fit shown in Fig. 5(*c*), the range of unique displacements required by each hinge in a pattern is reduced. This has the benefit of reducing the number of novel hinges which are required and can significantly simplify the design work required for a pattern.

4.1 Maximum Relative Displacement. From this model, it can be seen that the maximum magnitude of displacement is intuitively at the outermost edge of the outermost panel, such as the example shown in Fig. 2(*d*).

Color scaled heat maps are used in Fig. 6 to visually convey the effect the different parameters have on the maximum displacement of a rolled pattern. Fig. 6 shows every combination of the four parameters mentioned in Section 3. It should be noted that the units of the input parameters depend on the specific use case; for this reason the values in these charts are unitless. The purpose of these charts is to visually show the relationship between the parameters and maximum slippage rather than quantify specific displacement amounts for future replication. For this reason the actual output values of each configuration are not shown. The heat maps show a positive correlation between increased panel thickness and increased slippage, as well as increased strip length and increased slippage. There is a negative correlation, on the other hand, between both the minimum bend radius and number of panels with the amount of slippage that occurs. Inspection of the heat maps shows that the thickness of each panel has the largest relative effect on the maximum slippage that occurs in the pattern. Designers of rolled gossamer structures can use these heat maps as tools to visualize the relative magnitudes and directions each parameter will have on the slippage of panels when making design decisions.

4.2 Linear Fit Relationships. The relationships between each parameter and the slope of the slippage are similar to those of the maximum displacement, in that there is a positive correlation between the thickness and length with increasing slippage, and a negative correlation between the number of panels and the minimum bend radius with increasing slippage. One of the main differences between the effects on the maximum displacement and the slope of the slippage for each hinge location is the rate at which they change with each parameter. For example, it can be seen by comparing Figs. 6(*a*) and 7(*a*), Figs. 6(*d*) and 7(*d*), and Figs. 6(*e*) and 7(*e*), that the number of panels has a greater impact on the slope of the slippage at each hinge location than it does on reducing the maximum slippage in the design.

5 Implementation

To validate the accuracy of the model, an example prototype was made and compared with simulated results, using the double roll model. While the single exterior slip model has been discussed so far, the double roll was chosen for this prototype to demonstrate an example of an additional model. The prototype had the parameters $n = 6$, $r_{min} = 11mm$, $thickness = 0.2mm$, and $L = 600mm$, with 5 hinges along the length. This model is shown in Fig. 8(*a*), with the associated magnitude of slip for each hinge shown in Fig. 8(*b*). The prototype model was created using novel hinges which allow for rotation (during folding) and translation (for the slip during rolling), shown in Fig. 8(*d*). These hinges were designed specifically to accommodate the slip between panels, because all other rigid hinges would fail to allow for the sliding required between panels. These hinges are effectively cams which allow motion along the prescribed path. Note that all hinges in the prototype are the same size for simplicity; however, there are adverse effects from introducing a straight hinge into a curved section of material. Being able to accurately predict the maximum displacement at each hinge location allows designers to use the smallest hinges possible at that location, reducing these adverse effects. One method that could be used is to discretize the slip into 3-5 categories, such that each hinge location could use the smallest hinge which would also accommodate the slip required, rather than to create unique hinges for every hinge in the pattern. The prototype double roll is shown in Fig. 8(*c*). By measuring the linear displacement at each hinge, the results of the model can be evaluated. For the center hinge, shown in black, there was no measurable shifting as was expected. For the 3 hinges on each side at an intermediate location, shown in gray, the average shifting was 2.2 mm with a standard deviation of 0.9 mm. This corresponds to the predicted slip of 2.2 mm, with a 2.1% difference between the expected and actual values. The hinges at the outside edge, shown in white, had an average measured slip of 4.3 mm with a standard deviation of 0.7 mm. This corresponds to the predicted slip at the outside edge hinges of 4.3 mm, with a 0.64% difference between the expected and actual values. It should be noted that the friction in the hinges was non-trivial, and that by introducing a stiff linear segment into the rolled model, the results become less accurate. However, it is shown that the model predicted the hinge displacement, and that the methods presented in this paper show promise for use in the design of rolled gossamer structures.

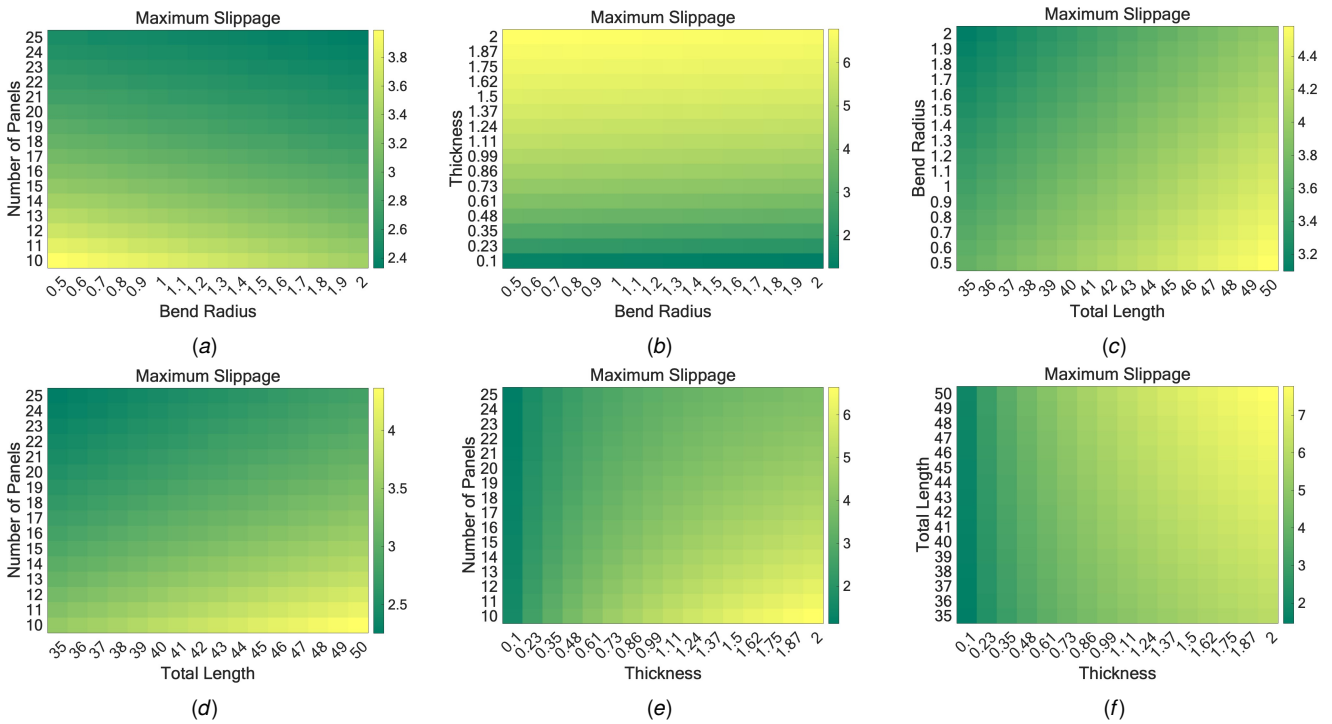

Fig. 6 Example heat maps showing how the maximum displacement changes for each combination of two parameters. For each combination, there are two parameters that change, and two parameters that are fixed. When fixed parameters are used in this example, there are thickness = 0.5, total length of each panel = 40, minimum bend radius = 1, and number of panels = 10.

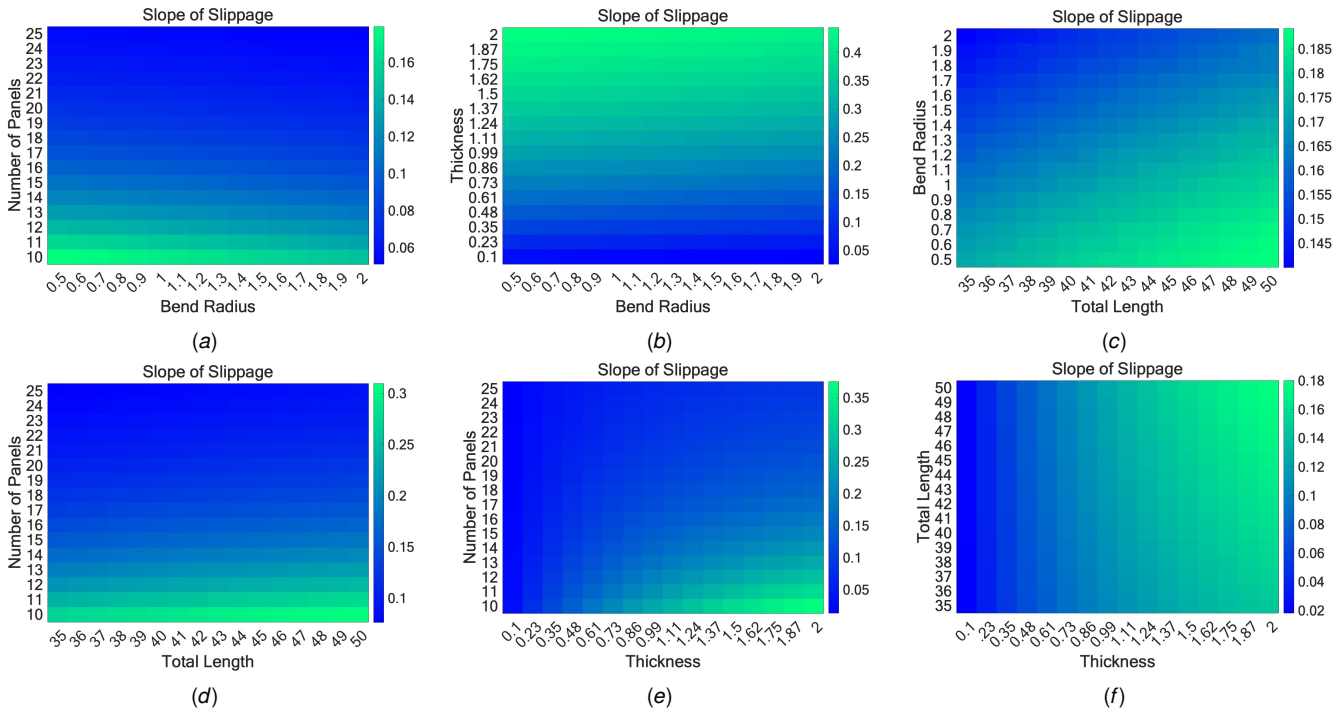

Fig. 7 Example heat maps showing how the slope of the linear fit changes for each combination of two parameters. For each combination, there are two parameters that change, and two parameters that are fixed. When fixed parameters are used in this example, there are thickness = 0.5, total length of each panel = 40, minimum bend radius = 1, and number of panels = 10.

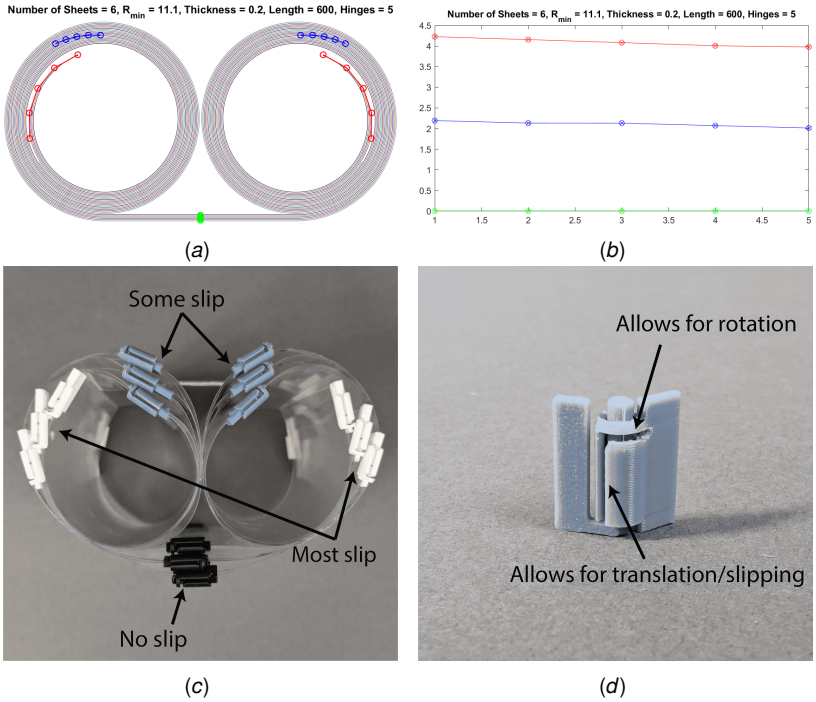

Fig. 8 Rolling model implementation with example hinges which can be used to accommodate slipping between panels. This model is shown in the open state in Fig.1. (a) Simulation model with the same parameters. Note that the red hinges in the model correspond to the white hinges in the prototype, the blue hinges in the model correspond to the gray hinges, and the green hinges in the model correspond to the black hinges in the prototype. Hinge colors were changed in the simulation to improve visibility. (b) Slip results for each hinge location in the simulation model. (c) Array in double rolled configuration. Note that the black hinges experience no slip, the gray hinges have some slip, and the white hinges on the outermost edges experience the most slip. (d) Simple hinge used to facilitate rotation and translational motion when stowed.

6 Conclusion

Gossamer structures are utilized in space applications to minimize stowed volume and maximize deployed surface area. Rolling the membranes that make up gossamer structures reduces wrinkles and creasing but requires relative slipping motion between panels. A numerical model was presented that determines the amount of slipping that occurs between rolled membrane strips, including how it varies across the array in response to changing the variables of thickness, length of the strips, number of panels, and minimum bend radius. This model was verified with a physical prototype, which incorporated novel hinges that accommodate for folding and sliding motion. This work is beneficial for future designers of rolled membrane structures, aiding them in the design of appropriate hinges to accommodate relative slipping motion between panels.

Acknowledgments

This paper was presented at the 2024 International Design Engineering Technical Conferences & Computers and Information in Engineering Conference (IDETC-CIE2024). This work has been funded by the Air Force Research Lab/U.S. Space Force, through award number FA9453-22-C-0013, and the Utah NASA Space Grant Consortium. Additional thanks are given to Brooklyn Coleman for her support of this work.

References

[1] 2024, "Online Index of Objects Launched into Outer Space," https://ourworldindata.org/grapher/yearly-number-of-objects-launched-into-outer-space?time=2003..latest
[2] Zhang, X., Kang, X., and Li, B., 2023, "Origami-Inspired Design of a Single-Degree-of-Freedom Reconfigurable Wing With Lockable Mechanisms," Journal of Mechanisms and Robotics, **16**(7), p. 071008.
[3] Guan, Y., Zhuang, Z., Zhang, Z., and Dai, J. S., 2023, "Design, Analysis, and Experiment of the Origami Robot Based on Spherical-Linkage Parallel Mechanism," Journal of Mechanical Design, **145**(8), p. 081701.
[4] Chen, F. and Aukes, D. M., 2023, "Direct Encoding of Tunable Stiffness Into an Origami-Inspired Jumping Robot Leg," Journal of Mechanisms and Robotics, **16**(3), p. 031012.
[5] Xing, D. and You, Z., 2023, "Origami Claw Tessellation and Its Stacked Structure," Journal of Mechanisms and Robotics, **16**(1), p. 011001.
[6] Yan, S., Song, K., Wang, X., Li, J., Ma, Z., and Zhou, X., 2024, "An Origami-Enabled Soft Linear Actuator and Its Application on a Crawling Robot," Journal of Mechanisms and Robotics, **17**(1), p. 011002.
[7] Howell, L. L., 2001, *Compliant Mechanisms*, Wiley.
[8] Branz, F. and Francesconi, A., 2023, "Compliant joint to reduce docking loads between CubeSats," Acta Astronautica, **205**, pp. 153–162.
[9] Liang, J., Zhang, X., Zhu, B., Zhang, H., and Wang, R., 2023, "Topology Optimization Method for Designing Compliant Mechanism With Given Constant Force Range," Journal of Mechanisms and Robotics, **15**(6), p. 061008.
[10] 1994, *Dimensional Synthesis of Compliant Constant-Force Slider Mechanisms*, Vol. 23rd Biennial Mechanisms Conference: Machine Elements and Machine Dynamics of International Design Engineering Technical Conferences and Computers and Information in Engineering Conference.
[11] McGowan, P. and Hao, G., 2022, "Design of a Morphing Compliant Mechanism With Separate Gripping and Retraction Modes Using a Single Actuation," Journal of Mechanisms and Robotics, **15**(1), p. 015002.

[12] Jenkins, C. H., 2001, *Gossamer spacecraft: membrane and inflatable structures technology for space applications*, American Institute of Aeronautics.
[13] Chandra, M., Kumar, S., Chattopadhyaya, S., Chatterjee, S., and Kumar, P., 2021, "A review on developments of deployable membrane-based reflector antennas," Advances in Space Research, **68**(9), pp. 3749–3764.
[14] Arya, M., Lee, N., and Pellegrino, S., 2016, "Ultralight structures for space solar power satellites," *3rd AIAA Spacecraft Structures Conference*, p. 1950.
[15] Fang, H., Lou, M., Huang, J., Hsia, L.-M., Quijano, U., Pelaez, G., and Svolopoulos, V., 2004, "Development of a 7-meter inflatable reflectarray antenna," *45th AIAA/ASME/ASCE/AHS/ASC Structures, Structural Dynamics & Materials Conference*, p. 1502.
[16] Seefeldt, P., Spietz, P., Sproewitz, T., Grundmann, J. T., Hillebrandt, M., Hobbie, C., Ruffer, M., Straubel, M., Tóth, N., and Zander, M., 2017, "Gossamer-1: Mission concept and technology for a controlled deployment of gossamer spacecraft," Advances in Space Research, **59**(1), pp. 434–456.
[17] Ruggiero, E. J. and Inman, D. J., 2006, "Gossamer spacecraft: recent trends in design, analysis, experimentation, and control," Journal of Spacecraft and Rockets, **43**(1), pp. 10–24.
[18] Furuya, H., Mori, O., Sawada, H., Okuizum, N., Shirasawa, Y., Natori, M., Miyazaki, Y., and Matunaga, S., 2011, "Manufacturing and Folding of Solar Sail'IKAROS'," *52nd AIAA/ASME/ASCE/AHS/ASC Structures, Structural Dynamics and Materials Conference 19th AIAA/ASME/AHS Adaptive Structures Conference 13t*, p. 1967.
[19] Arya, M., Hodges, R., Sauder, J. F., Horst, S., Mobrem, M., Pedivellano, A., Wen, A., Truong, A., and Pellegrino, S., 2021, *Lightweight Composite Reflectarray that can be Flattened, Folded, and Coiled for Compact Stowage*, Aerospace Research Central, Chap. 1, p. 17.
[20] Arya, M., Sauder, J. F., Hodges, R., and Pellegrino, S., 2019, *Large-Area Deployable Reflectarray Antenna for CubeSats*, Aerospace Research Central, Chap. 1, p. 12.
[21] Ruhl, L. E. and Wiens, M. T., 2023, "Deployable system with flexible membrane," US Patent 11,724,828.
[22] Tang, Y., Guo, H., Liu, R., and Deng, Z., 2023, "Space membrane wrinkle analytical model based on piecewise stress field," Thin-Walled Structures, **189**, p. 110869.
[23] Arya, M., Lee, N., and Pellegrino, S., 2015, "Wrapping thick membranes with slipping folds," *2nd AIAA Spacecraft Structures Conference*, p. 0682.
[24] Arya, M., Lee, N., and Pellegrino, S., 2017, "Crease-free biaxial packaging of thick membranes with slipping folds," International Journal of Solids and Structures, **108**, pp. 24–39.

List of Figures